

Universal conductance of a \mathcal{PT} -symmetric Luttinger liquid after a quantum quench

Cătălin Pașcu Moca^{1,2,*} and Balázs Dóra³

¹*MTA-BME Quantum-Dynamics and Correlations Research Group, Eötvös Loránd Research Network (ELKH), Budapest University of Technology and Economics, 1521 Budapest, Hungary*

²*Department of Physics, University of Oradea, 410087, Oradea, Romania*

³*Department of Theoretical Physics and MTA-BME Lendület Topology and Correlation Research Group, Budapest University of Technology and Economics, 1521 Budapest, Hungary*



(Received 3 December 2020; revised 29 August 2021; accepted 7 September 2021; published 17 September 2021)

We study the nonequilibrium dynamics and transport of a \mathcal{PT} -symmetric Luttinger liquid (LL) after an interaction quench. The system is prepared in domain wall initial state. After a quantum quench to spatially homogeneous, \mathcal{PT} -symmetric LL, the domain wall develops into a flat central region that spreads out ballistically faster than the conventional Lieb-Robinson maximal speed. By evaluating the current inside the regular light cone, we find a universal conductance e^2/h , insensitive to the strength of the \mathcal{PT} -symmetric interaction. On the other hand, by repeating the very same time evolution with a Hermitian LL Hamiltonian, the conductance is heavily renormalized by the Hermitian interaction as e^2/hK with K the LL parameter. Our analytical results are tested numerically, confirming the universality of the conductance in the non-Hermitian realm.

DOI: [10.1103/PhysRevB.104.125124](https://doi.org/10.1103/PhysRevB.104.125124)

I. INTRODUCTION

An important class of systems described by non-Hermitian Hamiltonians has emerged recently in quantum physics. Such models exhibit several exciting new phenomena such as exceptional point [1–6], non-Hermitian skin effect with the majority of eigenstates localized at the boundaries [7,8], topological transitions [9–11], and anomalous transport behavior [12–14] to mention a few. In general, a non-Hermitian Hamiltonian can arise naturally as the backaction to continuous monitoring and controlled post selection measurement that suppress the quantum jump processes [15]. Examples include inelastic one and two body losses in ultracold atomic lattices [16–19]. As such systems are under continuous surveillance, their state evolves in time under nonequilibrium conditions.

Among the non-Hermitian models, \mathcal{PT} -symmetric systems play a special role [20,21]. Such non-Hermitian Hamiltonians remain invariant with respect to the simultaneous action of the parity-inversion (P) and time reversal symmetry (T). These are the closest to Hermitian quantum mechanics in terms of having a real spectrum for unbroken \mathcal{PT} symmetry, therefore the conventional methods of statistical physics can be applied.

In this context, a key issue concerns the spreading of correlations captured by the typical light-cone effect following a quench [22]. It has been shown by Lieb and Robinson [23] that in Hermitian systems with short range interactions a maximal velocity for spreading the information does exist. On the other hand, in the non-Hermitian realm this maximum boundary is exceeded, as higher supersonic modes are developed [24], traveling with velocities that are multiples of the regular Lieb-Robinson sound velocity [25].

So far, the transport and dynamics following a quantum quench have been studied thoroughly in Hermitian models. A variety of different models have been considered, which can be framed into two main classes: The first consists of nonequilibrium dynamics in spatially homogeneous systems such as in spin- $\frac{1}{2}$ XXZ chain [26–28] or Hubbard chains [29–31]. In the second class the initial state is spatially inhomogeneous. Relevant examples are domain wall structures in XXZ models [32–35] or systems featuring local impurities [36–38]. In a previous publication [25] we have analyzed the behavior after the quantum quench in a homogeneous \mathcal{PT} -symmetric Luttinger liquid (LL) and found that the typical LL behavior is preserved in the long time limit, but at short times, the nonunitary evolution generates supersonic modes.

Transport in a LL has long been investigated. In a clean LL, the conductance was found to be strongly renormalized by the interaction [39]. However, it was found later that in an ideal LL connected to leads [40–42], the dc conductance depends only on the properties of the leads of a quantum wire containing a Luttinger liquid, and is given by the conductance quantum, e^2/h per spin orientation, regardless of the interactions in the wire.

The purpose of this paper is to extend the previous analysis and investigate the quench dynamics and the universality of transport in a non-Hermitian Luttinger liquid initially prepared in a domain wall state [43]. To make contact with the conventional condensed matter settings, here we discuss the electronic transport, but our theory applies as well to particle transport in neutral systems [44], e.g., cold atoms [45,46]. Our findings indicate that, similar to the homogeneous configuration [25], the supersonic modes are visible in the density $n(x, t)$ or the current $j(x, t)$ profiles as well. Surprisingly, inside the regular light cone, at long enough times for the system to stabilize, a nonequilibrium steady state is developing

*mocop@uoradea.ro

with a flowing current of a *constant* magnitude, irrespective of the strength of the interaction, corresponding to a universal conductance

$$G = \frac{e^2}{h}, \quad (1)$$

similar to the case of noninteracting spinless fermions. This occurs due to dissipation in much the same way as it occurs in Hermitian LL setup due to dissipation in the leads [40]. However, the basic difference is that dissipation takes place already within the LL due to the imaginary interaction in our case, even in the absence of leads. As non-Hermitian Hamiltonians naturally follow from open quantum systems, thus exchange with some external environment, the imaginary interaction could play the role of the reservoirs. It is important to keep in mind that this interaction produces also LL behavior [25] with fractional power law exponents. Furthermore, by time evolving the same initial state with a *Hermitian* LL Hamiltonian, the long time conductance of this nonequilibrium setting is e^2/hK with K the Luttinger liquid parameter [39], which keeps track of all interaction effects. To verify our analytical results we investigate numerically the nonequilibrium dynamics in a non-Hermitian lattice model using the time evolving block decimation (TEBD) algorithm [47–49], and we find perfect agreement with the bosonization results.

II. NON-HERMITIAN QUENCH PROTOCOL

We consider a global quench [50] in which the initial LL state displays a domain wall density profile [32,34,51,52], similar to the one obtained by joining two semi-infinite systems that are initially kept at different chemical potentials. Here we consider a symmetric configuration with a position dependent chemical potential of the form $\mu(x) = \mu_0 \operatorname{sgn}(x)$. Such a domain wall state can be realized experimentally in cold atoms setups [53–55] by, e.g., using a magnetic field gradient.

For such a system the ground state can be constructed exactly, and in the bosonic language it corresponds to the ground state of the shifted quantum harmonic oscillator Hamiltonian [39]

$$H_{\text{inh}} = \sum_{q \neq 0} \omega_q [b_q^\dagger b_q - \lambda_q (b_q^\dagger + b_q)], \quad (2)$$

where $\omega_q = v|q|$ is the energy of the bosonic excitations, b_q the annihilation operator for the density waves, and $\lambda_q = \mu_q/v\sqrt{2\pi|q|L}$ is a characteristic scale for the displacement of the ground state, with μ_q , the Fourier transform of the chemical potential profile $\mu(x)$. The Hamiltonian (2) can be diagonalized exactly in terms of the shifted bosonic operators a_q , defined as $a_q = b_q - \lambda_q$, which allows us to construct the GS as

$$|\Psi_0\rangle = \prod_q e^{-\frac{|\lambda_q|^2}{2}} e^{-\lambda_q b_q^\dagger} |0\rangle, \quad (3)$$

where $|0\rangle$ is the vacuum state for the b_q operators, $b_q|0\rangle = 0$. The vacuum state $|0\rangle$ contains no bosonic excitations and represents the GS of the homogeneous setup. The ground state $|\Psi_0\rangle$ represents the vacuum state for the a_q operators, $a_q|\Psi_0\rangle = 0$, and by construction it is properly normalized,

$\langle\Psi_0|\Psi_0\rangle = 1$. At $t = 0$, the Hamiltonian governing the evolution of the system suddenly changes from H_{inh} to a non-Hermitian PT-symmetric Hamiltonian H by switching on the interaction and turning off the chemical potential, $\mu(x) = \mu(x)\Theta(-t)$. Following the quench, the evolution is governed by the Hamiltonian

$$H = \sum_{q \neq 0} \omega_q b_q^\dagger b_q + \frac{ig_q}{2} [b_q b_{-q} + b_q^\dagger b_{-q}^\dagger]. \quad (4)$$

The Hamiltonian H is similar to an interacting LL but with an imaginary interaction ig_q instead. In general we use the parametrization $g_q = g_2|q|$ to describe the strength of the interaction. Although the Hamiltonian is non-Hermitian, as long as $g_2 < v$, the energy spectrum of H remains real as $\tilde{v}|q|$ with $\tilde{v} = \sqrt{v^2 + g_2^2}$ and H belongs to the PT-symmetrical models [56]. For larger g_2 , the system develops an instability [25].

A. Density and current profile

Following the quench, the time evolution of the conventional [39] density and the current profiles are

$$\begin{bmatrix} n(x, t) \\ j(x, t) \end{bmatrix} = -\frac{1}{\pi \mathcal{N}(t)} \langle \Psi(t) | \begin{bmatrix} \partial_x \phi(x) \\ \partial_x \theta(x) \end{bmatrix} | \Psi(t) \rangle, \quad (5)$$

where $|\Psi(t)\rangle = e^{-iHt} |\Psi_0\rangle$ describes the nonunitary time evolution on the initial wave function $|\Psi_0\rangle$ with Hamiltonian (4), and $\mathcal{N}(t) = \langle \Psi(t) | \Psi(t) \rangle$ is the norm of the wave function, while $\phi(x)$ and $\theta(x)$ are the regular LL fields, defined in terms of the b_q operators [39], and satisfying the regular commutation relations $[\partial_x \theta(x), \phi(y)] = i\pi \delta(x - y)$. Equation (5) is the conventional definition of the current and density. In our non-Hermitian setting, they only satisfy a continuity equation at the expense of introducing an additional source term, arising from the non-Hermitian term in Eq. (4), i.e., from interaction with the environment. Details on the continuity equation are discussed in Appendix A. In general, for a Hermitian Hamiltonian governing the dynamics, the wave function is properly normalized to 1, i.e., $\mathcal{N}(t) = 1$, while in the non-Hermitian realm this is no longer true, and the norm explicitly depends on time.

B. Initial density

The time and spatial evolution of the density profile $n(x, t)$ is captured by Eq. (5). At $t = 0$, we can calculate the initial profile of the local density as well. It can be shown that it is modeled by the spatial dependence of the chemical potential $\mu(x)$. To show that, we express the Luttinger field $\phi(x)$ in terms of the a_q operators as $\phi(x) = \phi_a(x) + \delta\phi(x)$, where $\phi_a(x)$ has the usual form [39]

$$\phi_a(x) = \phi_h(x) - \frac{i\pi}{L} \sum_{q \neq 0} \sqrt{\frac{L|q|}{2\pi}} \frac{1}{q} e^{-iqx} (a_q^\dagger + a_{-q}), \quad (6)$$

where $\phi_h(x) = -(N_L + N_R)\frac{\pi x}{L}$ represent the background local field and $\delta\phi(x)$ is the inhomogeneity induced by the chemical potential

$$\delta\phi(x) = \frac{2i\pi}{L} \sum_{q \neq 0} \sqrt{\frac{L|q|}{2\pi}} \frac{1}{q} e^{-iqx} \lambda_q. \quad (7)$$

The initial density profile can be evaluated as

$$n_i(x) = -\frac{1}{\pi} \langle \Psi_0 | \partial_x \phi(x) | \Psi_0 \rangle, \quad (8)$$

with the expectation value taken with respect to the ground state of H_{inh} given in Eq. (2). Taking into account that $|\Psi_0\rangle$ is the vacuum state for the a_q operators, it immediately implies that

$$-\frac{1}{\pi} \langle \Psi_0 | \partial_x \phi_a(x) | \Psi_0 \rangle = -\frac{1}{\pi} \langle \Psi_0 | \partial_x \phi_b(x) | \Psi_0 \rangle = n_0, \quad (9)$$

with $n_0 = (N_L + N_R)/L$ representing the homogeneous density background. The inhomogeneous contribution in Eq. (7) is Fourier transformed back to the real space, and the initial density profile is simply

$$n_{\text{inh}}(x, t = 0) = \frac{1}{\pi v} \mu(x) + n_0. \quad (10)$$

Equation (10) shows that the profile of the density in the initial state is determined exclusively by the chemical potential and follows exactly its shape. Notice that in deriving Eq. (10) no particular shape for $\mu(x)$ has been considered so the result is valid for any spatial distribution of the chemical potential. At the same time, the initial current is zero.

C. Density profile following the quench

Following the strategy put forward in Ref. [25], we can evaluate $n(x, t)$ and $j(x, t)$ using the pseudo-Heisenberg time evolution approach. Let us illustrate the derivation in terms of the density profile; the derivation for the current profile is similar with the proper replacement $\phi(x) \rightarrow \theta(x)$ in Eq. (5) and will be discussed in Sec. IID. We first introduce the pseudo-Heisenberg time dependent fields $\psi(x, t > 0) = e^{iHt} \psi(x) e^{-iHt}$ and the non-Hermitian forward and backward time evolution operator $U(t) = e^{iH^+t} e^{-iHt}$ in terms of which $n(x, t)$ becomes

$$n(x, t) = -\frac{1}{\pi} \frac{\langle \Psi_0 | U(t) \partial_x \phi(x, t) | \Psi_0 \rangle}{\langle \Psi_0 | U(t) | \Psi_0 \rangle}. \quad (11)$$

In any typical Hermitian problem $U_H(t) = 1$, but since $[H, H^+] \neq 0$, it follows that $U(t) \neq 1$ for the non-Hermitian evolution. Notice that the time dependent fields are not constructed in the regular way as in the Heisenberg picture but in a modified pseudo-Heisenberg way which is more suitable for our calculations. Using this construction, $U(t)$ is rewritten as

$$U(t) = \prod_{q>0} e^{C_+(q,t)K_+(q)} e^{C_0(q,t)K_0(q)} e^{C_-(q,t)K_-(q)}, \quad (12)$$

in terms of the generators for the $SU(1, 1)$ algebra $K_0(q) = \frac{1}{2}(b_q^\dagger b_q + b_{-q} b_{-q}^\dagger)$, $K_+(q) = b_q^\dagger b_{-q}^\dagger$, and $K_-(q) = b_{-q} b_q$. Using the construction in Eq. (12) and the standard Baker-Hausdorff expressions, the time dependence of the norm of the wave function is evaluated as

$$\mathcal{N}(t) = \prod_{q>0} \frac{\tilde{\omega}_q^2}{\tilde{\omega}_q^2 - 2g^2 \sin^2 \tilde{\omega}_q t} e^{2|\lambda_q|^2 \frac{g\tilde{\omega}_q \sin 2\tilde{\omega}_q t + 2g^2 \sin^2 \tilde{\omega}_q t}{\tilde{\omega}_q^2 - 2g^2 \sin^2 \tilde{\omega}_q t}}. \quad (13)$$

Details on the derivation of Eq. (13) are discussed in Appendix B. To evaluate the numerator in Eq. (11) and calculate the time dependence of the density profile, it is required to know the time evolution of the $b_q(t)$ operators. Their time dependence relies explicitly on the form of the final Hamiltonian and can be expressed exactly in terms of two Bogoliubov

coefficients $u_q(t)$ and $v_q(t)$ to which the time dependence is completely transferred. In evaluating $n(x, t)$ and $j(x, t)$ we normal order the product of various b_q and b_q^\dagger operators. The expressions for the Bogoliubov coefficients $u_q(t)$ and $v_q(t)$ are derived in Appendix C.

With the exact analytical expressions for the coefficients $u_q(t)$ and $v_q(t)$ at hand we can derive exact expressions for the time dependence of the density and current profiles following the quench by using Eq. (5). Introducing the notation $\beta_q(x) = -\frac{\pi}{L} e^{-iqx} e^{-\alpha|q|/2} \sqrt{\frac{L|q|}{2\pi}}$, for the overall prefactor in the $\theta(x)$ and $\phi(x)$ fields and separating the contributions coming from the creation and annihilation operators we can write $\partial_x \phi(x, t) = \partial_x \phi_-(x, t) + \partial_x \phi_+(x, t)$, with

$$\partial_x \phi_+(x, t) = \sum_{q>0} (u_q^*(t) + v_q(t)) (\beta_q(x) b_q^\dagger + \beta_q^*(x) b_{-q}^\dagger)$$

$$\partial_x \phi_-(x, t) = \sum_{q>0} (u_q(t) - v_q(t)) (\beta_q(x) b_{-q} + \beta_q^*(x) b_q).$$

In evaluating $n(x, t)$ we follow the same strategy as the one in computing the norm $\mathcal{N}(t)$ and normal ordering the product of various b_q and b_q^\dagger operators.

The piece $\partial_x \phi_-(x, t)$ gives a partial contribution to the regular light cone. When evaluating $n_-(x, t)$, the norm drops out and we obtain

$$\begin{aligned} n_-(x, t) &= \frac{1}{2\pi L \tilde{v}} \sum_{q \neq 0} (u_q(t) - v_q(t)) e^{-iqx} e^{-\alpha|q|/2} h_q \\ &\simeq \frac{1}{4\pi \tilde{v}} (\mu(x - \tilde{v}t) + \mu(x + \tilde{v}t)). \end{aligned} \quad (14)$$

The contribution from $\partial_x \phi_+(x, t)$ is more involved. Still, it can be brought into a compact expression of the form

$$\begin{aligned} n_+(x, t) &= \frac{1}{2\pi L} \sum_{q>0} (u_p^*(t) + v_p(t)) \\ &\times \frac{\tilde{\omega}_q^2 - u_p(t) \tilde{\omega}_q g \sin \tilde{\omega}_q t}{\tilde{\omega}_q^2 - 2g^2 \sin^2 \tilde{\omega}_q t} 2 \sin(qx) e^{-\alpha|q|} \mu_q. \end{aligned} \quad (15)$$

This part contributes to the regular light cone but also the supersonic modes. To separate the two contributions we expanded $n_+(x, t)$ in Taylor series in $\sin^2 \tilde{\omega}_q t$. The zeroth order term contributes to the regular light cone while all the other higher order terms contribute to the supersonic modes. We then have $n(x, t) = n_r(x, t) + n_s(x, t)$ with

$$n_r(x, t) = \frac{1}{2\pi \tilde{v}} (\mu(x - \tilde{v}t) + \mu(x + \tilde{v}t)), \quad (16)$$

showing the development of the regular light cone after the quench and n_s describing the supersonic modes

$$\begin{aligned} n_s(x, t) &= \frac{1}{2\pi L \tilde{v}} \sum_{q>0} \sum_{n=1}^{\infty} (u_p^*(t) + v_p(t)) \\ &\times \left(1 - u_p(t) \frac{g \sin \tilde{\omega}_q t}{\tilde{\omega}_q} \right) \\ &\times \left(\frac{\sqrt{2} g \sin \tilde{\omega}_q t}{\tilde{\omega}_q} \right)^{2n} 2i \sin(qx) e^{-\alpha|q|} \mu_q. \end{aligned} \quad (17)$$

Notice that when the model is Hermitian, all the terms $\sim \sin \tilde{\omega}_q t$ cancel and the contribution $n_s(t)$ vanishes. For a given profile of the initial chemical potential $\mu(x)$, the various integrals in Eq. (17) can be computed term by term in the perturbative expansion. If we consider the simplest chemical potential profile corresponding to a steplike function of the form $\mu(x) = \mu_0 \text{sgn}(x)$, the corresponding Fourier transform is $\mu_p \propto \mu_0 \frac{2i}{p}$, and the integrals (sums) in Eq. (17) can be performed order by order in the perturbation theory in g_2/\tilde{v} to reveal to supersonic modes.

D. Current profile following the quench

Once the chemical potential is turned off, and the interaction is quenched, the initial domain wall induces a change in the local density and a complementary current flows across the domain wall. Furthermore, the domain wall extends and transforms into a central region inside the light cone characterized by a steady current. The current density can be evaluated in terms of the $\theta(x, t)$ field

$$\theta(x) = \frac{i\pi}{L} \sum_{q \neq 0} \sqrt{\frac{L|q|}{2\pi}} \frac{1}{|q|} e^{-iqx} (b_q^\dagger - b_{-q}), \quad (18)$$

as

$$j(x, t) = -\frac{1}{\pi} \frac{\langle \Psi_0(t) | \partial_x \theta(x) | \Psi_0(t) \rangle}{\mathcal{N}(t)}, \quad (19)$$

which allows us to compute the current profile in a similar fashion as we computed the local density. Performing similar steps we can express the total current as a sum $j(x, t) = j_r(x, t) + j_s(x, t)$ where the regular light cone contribution is

$$j_r(x, t) = \frac{1}{2\pi} (\mu(x - \tilde{v}t) - \mu(x + \tilde{v}t)), \quad (20)$$

and a non-Hermitian part that can be again expressed as a power series of the form

$$\begin{aligned} j_s(x, t) &= \frac{1}{2\pi L} \sum_{q>0} \sum_{n=1}^{\infty} (u_p(t) + v_p^*(t)) \\ &\times \left(1 - u_p(t) \frac{g \sin \tilde{\omega}_q t}{\tilde{\omega}_q} \right) \\ &\times \left(\frac{\sqrt{2} g \sin \tilde{\omega}_q t}{\tilde{\omega}_q} \right)^{2n} 2 \cos(qx) e^{-\alpha|q|} \mu_q, \end{aligned} \quad (21)$$

an expression that allows us to compute the current order by order in the perturbation theory in a manner similar to Eq. (17).

Gathering the results for the density and the current profiles, following the quench we can express them in a compact form. For the regular contribution responsible for the development of the regular light cone we have

$$\begin{bmatrix} n_r(x, t) \\ j_r(x, t) \end{bmatrix} = \frac{1}{2\pi} \begin{bmatrix} \frac{1}{\tilde{v}} & \frac{1}{\tilde{v}} \\ 1 & -1 \end{bmatrix} \begin{bmatrix} \mu(x - \tilde{v}t) \\ \mu(x + \tilde{v}t) \end{bmatrix}. \quad (22)$$

The other contributions, explicitly given in Eqs. (17) and (21) for $n_s(x, t)$ and $j_s(x, t)$ are more involved and describe the supersonic modes. Their time dependences are responsible for the supersonic modes and the formation of multiple light cones. Although it displays a strong spatial and temporal

behavior in general, it vanishes in the long time limit, $t \rightarrow \infty$, close to the center $x \sim 0$, implying that only the regular contribution $j_r(x, t)$ controls the transport properties in the steady state.

E. Post-quench conductance

Following the quench, the initial domain wall develops into a central region, delimited by the boundaries of the light cone. This region extends ballistically in time in both directions with the light speed velocity $\pm \tilde{v}$. In a weak sense, in this region a local steady state is formed as the density equilibrates, but, due to the chemical potential drop, a particle current flows continuously. This allows us to define the conductance that characterizes the nonequilibrium steady state across the interface

$$G = \frac{1}{2} \left. \frac{d j(x, t)}{d \mu_0} \right|_{\substack{x \rightarrow 0 \\ \mu_0 \rightarrow 0}}. \quad (23)$$

The regular contribution to the current gives a contribution to the conductance $G_r = G_0$ with $G_0 = e^2/h$ the conductance quantum upon reinserting original units. Interestingly, the anomalous contribution to the current from supersonic modes vanishes in the long time limit, implying $G_s = 0$, and the conductance acquires an universal value given by Eq. (1) irrespective of the strength of the interaction. This conductance is the unitary conductance of a single spinless channel and, at the same time, it corresponds to the conductance of a LL connected to leads [40,41]. In both these cases, the correlations are characterized by fractional LL exponents [25] and the quantized conductance occurs due to dissipation. However, dissipation occurs within the LL due to imaginary interaction in our case, while it takes place within the leads in the conventional Hermitian setting [40,41]. This is to be contrasted to the post-quench conductance of a Hermitian LL, characterized by the Luttinger parameter [39] K , given by $G_H = G_0/K$, thus in case of the unitary evolution the conductance strongly depends on the interaction strength [57] from the ensuing nonequilibrium state.

III. LATTICE MODEL

We corroborate our analytical results with a numerical analysis. For that we investigate numerically all the features that we have addressed so far, such as the formation of the light cone, the presence of the supersonic modes, and most importantly we calculate the conductance across the interface following the quench in a one-dimensional spinless lattice model. The initial state is constructed as a matrix product state by performing density matrix renormalization group (DMRG) calculations [58] on the noninteracting spinless Hamiltonian

$$H_{\text{inh}}^{(\text{lat})} = \sum_{m=1}^N \mu_m c_m^\dagger c_m + \sum_{m=1}^N \frac{J}{2} (c_{m+1}^\dagger c_m + \text{H.c.}), \quad (24)$$

subject to a site dependent chemical potential of the form $\mu_m = \mu_0 \text{sgn}(m - N/2)$, realizing a domain wall. Here c_m^\dagger are the creation operators at site m along the chain. In our calculations we fixed the chain length to $N = 100$, while J , the nearest neighbor hopping, represents the energy unit.

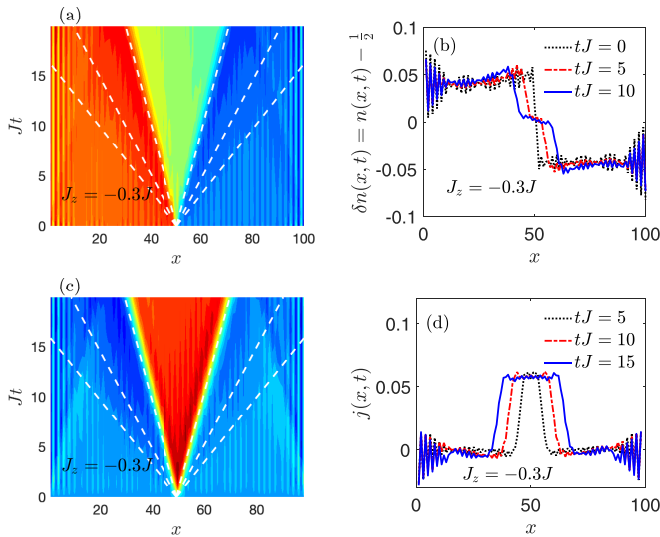


FIG. 1. (a) Formation of the regular light cone as well as the supersonic modes in the density profile $n(x, t)$ for $J_z = -0.3J$. (b) Cuts at a given time along the chain, displaying particles accumulation between the regular and supersonic light cones. (c) Density plot for the current $j(x, t)$. (d) Evolution of the current along the chain. In panels (a) and (c) the white dashed lines represent the world lines for the light cones.

The MPS wave function is then evolved in time using the TEBD algorithm [48,49], with a non-Hermitian evolution operator constructed from the Hamiltonian

$$H^{(\text{lat})} = \sum_{m=1}^N \frac{J + iJ_z}{2} (c_{m+1}^+ c_m + \text{H.c.}) - i \frac{J_z \pi}{2} n_{m+1} n_m, \quad (25)$$

where J_z is real and denotes the nearest neighbor interaction. This model possesses a complex spectrum and is not PT symmetric, but the low energy part of its spectrum can be considered real, which influences the early time dynamics [25]. When J_z is turned imaginary, $J_z \rightarrow -iJ_z$, the model becomes the regular XXZ Hermitian Heisenberg model, which is Bethe-Ansatz solvable [39] with a sound velocity $v_H \approx J + (1 - \pi^2/8)J_z^2/J$. It has a BKT [39] phase transition at $J_z/J = -2/(2 + \pi)$. On the other hand, the low energy excitations for the non-Hermitian version are sound waves with sound velocity $\tilde{v} \approx J + (\pi^2/8 - 1)J_z^2/J$. Figure 1(a) displays the density plot for the occupation $n(x, t)$ along the chain as a function of time. The regular light cone is clearly visible but also the formation of the second and third supersonic modes that propagates at velocities $v_n = n\tilde{v}$, $n = 2, 3$. The world lines for the light cones are displayed with dashed lines.

The formation of various fronts is also visible in the density plot displaying the current $j(x, t)$ as well. Furthermore, Figs. 1(b) and 1(d) present several cuts at fixed times along the chain for the density and current profiles. In the cuts representing $j(x, t)$ the formation of the plateau inside the light cone, displaying the region with the constant currents are clearly visible.

We compute the conductance numerically by using Eq. (23). For that, we find the stationary current at the interface in the long time limit, $tJ \sim 20$, for various initial

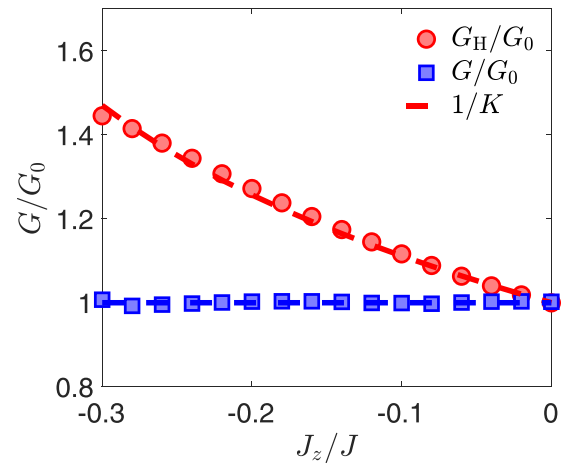


FIG. 2. The universal conductance of the PT non-Hermitian Luttinger model indicating the universal behavior predicted in Eq. (1) (blue symbols). The red symbols correspond to the conductance of the Hermitian interacting LL model, consisting in replacing $J_z \rightarrow -iJ_z$ in Eq. (25). The red dashed line represents the fit with the analytical expressions displayed in the legend. The initial state corresponds to a noninteracting model.

chemical potentials drops μ_0 and then take the derivative numerically. We perform an average over a time interval of the order of $2-3/J$ to remove the local oscillations sometimes visible in the current. For small enough μ_0 's the stationary currents depend linearly on the μ_0 , which allows us to extract the conductance as the slope of the current. The final result for the non-Hermitian conductance is displayed in Fig. 2. Irrespective of the value of the coupling strength J_z , the conductance remains universal and equal to the conductance quantum in perfect agreement with bosonization from Eq. (1). We note that Eq. (25) contains many other terms compared to Eq. (4), nevertheless gives the very same quantized conductance. We also display the results for the Hermitian evolution,

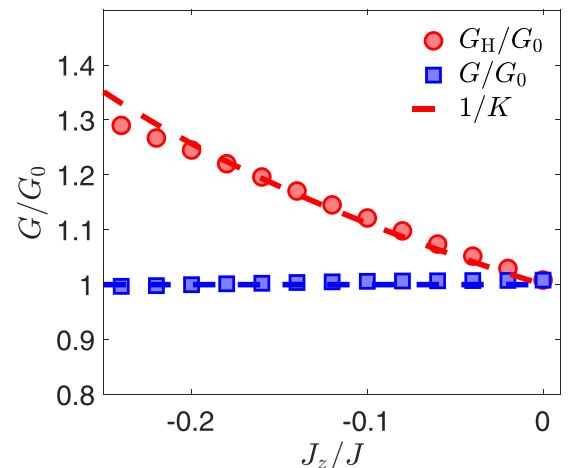


FIG. 3. Conductance of the PT non-Hermitian Luttinger model, when the initial state is a Hermitian interacting Luttinger liquid. The conductance remains universal when the system is quenched from an interacting state to a non-Hermitian model irrespective on the strength of the initial and post-quench interactions.

by replacing $Jz \rightarrow -iJz$ in Eq. (25) where the analytical prediction from Ref. [57] fits also perfectly.

Our analysis extends as well to the case where the initial state is the ground state of a Hermitian, interacting Luttinger liquid. Using TEBD we found that the conductance inside the light cone depends exclusively on the post-quench Hamiltonian and remains quantized when the system is quenched to the non-Hermitian Hamiltonian. The results for the conductance, when the system is quench from an interacting initial state, are displayed in Fig. 3 and indicates that the initial state has no effect on the conductance. Furthermore, irrespective of the strength of the initial or final interactions, the non-Hermitian dynamics following the quench displays a conductance that remains always universal.

IV. CONCLUSIONS

We study the nonequilibrium dynamics and transport of a PT-symmetric Luttinger liquid when the model is quenched from a domain wall initial state. Due to nonunitary time evolution, we identify the formation of supersonic modes on top of the regular light cone both in the density and current profiles after the quench. Most importantly, we find the universal value, e^2/h for the conductance at the interface, which is a very robust analytical result, benchmarked by the numerical simulations. The quantized conductance occurs due to dissipation within the LL from the PT-symmetric interaction. Moreover, for a unitary time evolution with a Hermitian Luttinger liquid Hamiltonian, the resulting nonequilibrium conductivity gets heavily renormalized by the interaction as e^2/hK . Our setup can in principle be realized in dissipative lattices [59,60] for which our predictions can be tested experimentally.

ACKNOWLEDGMENTS

This research is supported by the National Research, Development and Innovation Office - NKFIH within the Quantum Technology National Excellence Program (Project No. 2017-1.2.1-NKP-2017-00001), K119442, K134437 and by the Romanian National Authority for Scientific Research and Innovation, UEFISCDI, under Project No. PN-III-P4-ID-PCE-2020-0277.

APPENDIX A: ON THE CONTINUITY EQUATION

The continuity equation states that the local density can only change when local current flows or some external source or sink is present. A non-Hermitian system usually arises from some interaction with the environment, therefore the last terms are also expected in the continuity equation. A non-Hermitian Hamiltonian can always be written as $H = H_0 + iV$ with both H_0 and V being Hermitian. The expectation value of the local density n is

$$\langle n \rangle = \frac{\langle \Psi(t) | n | \Psi(t) \rangle}{\langle \Psi(t) | \Psi(t) \rangle}, \quad (\text{A1})$$

where $|\Psi(t)\rangle = e^{-iHt}|\Psi_0\rangle$. Then, the time derivative of this expectation value reads as [61]

$$\begin{aligned} \partial_t \langle n \rangle &= i \frac{\langle \Psi(t) | H^+ n - n H | \Psi(t) \rangle}{\langle \Psi(t) | \Psi(t) \rangle} \\ &\quad - i \frac{\langle \Psi(t) | n | \Psi(t) \rangle \langle \Psi(t) | H^+ - H | \Psi(t) \rangle}{\langle \Psi(t) | \Psi(t) \rangle \langle \Psi(t) | \Psi(t) \rangle} \\ &= i \langle [H, n] \rangle + \langle \{V, n\} \rangle - 2 \langle n \rangle \langle V \rangle, \end{aligned} \quad (\text{A2})$$

where $[,]$ and $\{, \}$ stand for the commutator and anticommutator, respectively. The first term on the right hand side represents the conventional term for Hermitian systems, the second term with the anticommutator stems from the non-Hermitian contribution, namely from the interaction with the environment, while the very last term originates from the explicit normalization of the wave function in Eq. (A1).

Putting all this together, the continuity equation in one dimension for a non-Hermitian system reads as

$$\partial_t \langle n \rangle + \partial_x \langle j \rangle = \langle \{V, n\} \rangle - 2 \langle n \rangle \langle V \rangle, \quad (\text{A3})$$

where the source term on the right hand side accounts for interaction with the environment [13]. This equation is satisfied by the density and current in Eq. (5).

APPENDIX B: NORM OF THE WAVE FUNCTION

The evaluation of the norm $\mathcal{N}(t)$ in Eq. (13) is done by using the expression for the evolution operator $U(t)$ from Eq. (12). Keeping in mind that $\lambda_q = -\lambda_{-q}$ is an antisymmetric function, the norm is cast in the following form

$$\begin{aligned} \mathcal{N}(t) &= \prod_{q>0} e^{-2|\lambda_q|^2} \langle 0 | e^{-\lambda_q^* (b_q - b_{-q})} e^{C_+(q,t) K_+(q)} \\ &\quad \times e^{C_0(q,t) K_0(q)} e^{C_-(q,t) K_-(q)} e^{-\lambda_q (b_q^\dagger - b_{-q}^\dagger)} | 0 \rangle. \end{aligned} \quad (\text{B1})$$

Here we need to compute the expectation value with respect to the initial state $|\Psi_0\rangle$ given in Eq. (3). In evaluating (B1), the strategy is to normal order the exponentials with the annihilation operators b_q to the right and the creation operators b_q^\dagger to the left. Let us discuss here the reordering of the last two exponents in (B1), as the rest of the calculation is conceptually the same. For that, we first expand the last exponential into Taylor series

$$e^{-\lambda_q (b_q^\dagger - b_{-q}^\dagger)} = \sum_{n=1}^{\infty} \frac{1}{n!} (-\lambda_q)^n (b_q^\dagger - b_{-q}^\dagger)^n. \quad (\text{B2})$$

Next, keeping in mind that $K_-(q, t) = b_{-q} b_q$, it can be readily shown using the Baker-Hausdorff formula that

$$\begin{aligned} e^{C_-(q,t) K_-(q)} b_q^\dagger &= (b_q^\dagger + C_-(q, t) b_{-q}) e^{C_-(q,t) K_-(q)} \\ e^{C_-(q,t) K_-(q)} b_{-q}^\dagger &= (b_{-q}^\dagger + C_-(q, t) b_q) e^{C_-(q,t) K_-(q)}. \end{aligned}$$

Performing the rotation for the whole series and reshaping the result back into an exponential form we obtain

$$\begin{aligned} \mathcal{N}(t) &= \prod_{q>0} e^{(C_-(q,t)-2)|\lambda_q|^2} \langle 0 | e^{-\lambda_q^* (b_q - b_{-q})} e^{C_+(q,t) K_+(q)} \\ &\quad \times e^{C_0(q,t) K_0(q)} e^{-\lambda_q (b_q^\dagger - b_{-q}^\dagger)} | 0 \rangle. \end{aligned} \quad (\text{B3})$$

Performing similar transformations to fully normal order the expression we obtain for the norm factor

$$\mathcal{N}(t) = \prod_{q>0} e^{\frac{C_0(q,t)}{2}} e^{(C_+(q,t)+C_-(q,t)-2+2e^{\frac{C_0(q,t)}{2}})|\lambda_q|^2}. \quad (\text{B4})$$

The exact expressions for the coefficients $C_{\pm,0}(q, t)$ can be obtained following the strategy discussed in Sec. II C. The final expressions are

$$\begin{aligned} C_0(q, t) &= -2 \ln \frac{\tilde{\omega}_q^2 - 2g^2 \sin 2\tilde{\omega}_q t}{\tilde{\omega}_q^2} \\ C_+(q, t) &= \frac{g(i\omega_q \sin \tilde{\omega}_q t + \tilde{\omega}_q \cos \tilde{\omega}_q t) \sin \tilde{\omega}_q t}{\tilde{\omega}_q^2 - 2g^2 \sin^2 \tilde{\omega}_q t} \\ C_-(q, t) &= C_+^*(q, t), \end{aligned} \quad (\text{B5})$$

which allows us to recover the expression for $\mathcal{N}(t)$ in Eq. (13). At $t = 0$, obviously $N = 1$ and the wave function is properly normalized.

APPENDIX C: TIME DEPENDENCE OF THE EVOLUTION OPERATORS

In this section we discuss the pseudo-Heisenberg time evolution of the annihilation/creation operators. Their time dependence is governed by $b_q(t) = e^{iHt} b_q e^{-iHt}$, which

results in a Heisenberg equation of the form

$$\partial_t b_q(t) = i[H, b_q(t)], \quad \partial_t b_q^\dagger(t) = i[H, b_q^\dagger(t)]. \quad (\text{C1})$$

Notice that the equation for $b_q^\dagger(t)$ is not recovered from the one for $b_q(t)$ simply by Hermitian conjugation. Computing the commutators with the Hamiltonian (4), we obtain

$$\begin{aligned} \partial_t b_q(t) &= -i\omega_q b_q(t) + g b_{-q}^\dagger(t) \\ \partial_t b_{-q}^\dagger(t) &= i\omega_q b_{-q}^\dagger(t) - g b_q(t). \end{aligned} \quad (\text{C2})$$

To solve this set of equations we start by searching for a general solution of the form

$$\begin{bmatrix} b_q(t) \\ b_{-q}^\dagger(t) \end{bmatrix} = \begin{bmatrix} u_q(t) & v_q(t) \\ -v_q^*(t) & u_q^*(t) \end{bmatrix} \begin{bmatrix} b_q \\ b_{-q}^\dagger \end{bmatrix}. \quad (\text{C3})$$

Such a solution is useful since time dependence is transferred to the Bogoliubov coefficients $u_q(t)$ and $v_q(t)$ entirely. Using the commutativity relation $[b_q, b_q^\dagger] = 1$, it follows that $|u_q(t)|^2 + |v_q(t)|^2 = 1$ and that they satisfy a differential equation similar to (C2). Finally the solution is captured by the expressions

$$u_q(t) = \cos \tilde{\omega}_q t - i \frac{\omega_q}{\tilde{\omega}_q} \sin \tilde{\omega}_q t, \quad v_q(t) = \frac{g}{\tilde{\omega}_q} \sin \tilde{\omega}_q t, \quad (\text{C4})$$

in terms of the renormalized excitation energy of the quasiparticles.

-
- [1] T. Stehmann, W. D. Heiss, and F. G. Scholtz, *J. Phys. A: Math. Gen.* **37**, 7813 (2004).
- [2] W. D. Heiss, *J. Phys. A: Math. Gen.* **37**, 2455 (2004).
- [3] M.-A. Miri and A. Alù, *Science* **363**, 42 (2019).
- [4] Ş. K. Özdemir, S. Rotter, F. Nori, and L. Yang, *Nat. Mater.* **18**, 783 (2019).
- [5] L. E. F. F. Torres, *J. Phys.: Mater.* **3**, 014002 (2020).
- [6] V. M. Martínez Alvarez, J. E. Barrios Vargas, and L. E. F. Torres, *Phys. Rev. B* **97**, 121401(R) (2018).
- [7] S. Yao and Z. Wang, *Phys. Rev. Lett.* **121**, 086803 (2018).
- [8] S. Longhi, *Phys. Rev. Research* **1**, 023013 (2019).
- [9] J. M. Zeuner, M. C. Rechtsman, Y. Plotnik, Y. Lumer, S. Nolte, M. S. Rudner, M. Segev, and A. Szameit, *Phys. Rev. Lett.* **115**, 040402 (2015).
- [10] T. E. Lee, *Phys. Rev. Lett.* **116**, 133903 (2016).
- [11] L. Zhou, Q.-h. Wang, H. Wang, and J. Gong, *Phys. Rev. A* **98**, 022129 (2018).
- [12] T. Eichelkraut, R. Heilmann, S. Weimann, S. Stützer, F. Dreisow, D. N. Christodoulides, S. Nolte, and A. Szameit, *Nat. Commun.* **4**, 2533 (2013).
- [13] H. Schomerus and J. Wiersig, *Phys. Rev. A* **90**, 053819 (2014).
- [14] S. Longhi, D. Gatti, and G. D. Valle, *Sci. Rep.* **5**, 13376 (2015).
- [15] Y. Ashida, S. Furukawa, and M. Ueda, *Phys. Rev. A* **94**, 053615 (2016).
- [16] A. Turlapov, A. Tonyushkin, and T. Sleator, *Phys. Rev. A* **68**, 023408 (2003).
- [17] N. Syassen, D. M. Bauer, M. Lettner, T. Volz, D. Dietze, J. J. García-Ripoll, J. I. Cirac, G. Rempe, and S. Dürr, *Science* **320**, 1329 (2008).
- [18] T. Tomita, S. Nakajima, I. Danshita, Y. Takasu, and Y. Takahashi, *Sci. Adv.* **3**, e1701513 (2017).
- [19] T. Tomita, S. Nakajima, Y. Takasu, and Y. Takahashi, *Phys. Rev. A* **99**, 031601(R) (2019).
- [20] C. M. Bender and S. Boettcher, *Phys. Rev. Lett.* **80**, 5243 (1998).
- [21] R. El-Ganainy, K. G. Makris, M. Khajavikhan, Z. H. Musslimani, S. Rotter, and D. N. Christodoulides, *Nat. Phys.* **14**, 11 (2018).
- [22] M. Cheneau, P. Barmettler, D. Poletti, M. Endres, P. Schauß, T. Fukuhara, C. Gross, I. Bloch, C. Kollath, and S. Kuhr, *Nature (London)* **481**, 484 (2012).
- [23] E. H. Lieb and D. W. Robinson, *Commun. Math. Phys.* **28**, 251 (1972).
- [24] Y. Ashida and M. Ueda, *Phys. Rev. Lett.* **120**, 185301 (2018).
- [25] B. Dóra and C. P. Moca, *Phys. Rev. Lett.* **124**, 136802 (2020).
- [26] F. Pollmann, M. Haque, and B. Dóra, *Phys. Rev. B* **87**, 041109(R) (2013).
- [27] M. Mestyán, B. Pozsgay, G. Takács, and M. A. Werner, *J. Stat. Mech.: Theory Exp.* (2015) P04001.
- [28] B. Schoenauer and D. Schuricht, *Phys. Rev. B* **100**, 115418 (2019).
- [29] M. Moeckel and S. Kehrein, *Phys. Rev. Lett.* **100**, 175702 (2008).

- [30] A. M. Läuchli and C. Kollath, *J. Stat. Mech.: Theory Exp.* (2008) P05018.
- [31] B. Bertini, E. Tartaglia, and P. Calabrese, *J. Stat. Mech.: Theory Exp.* (2017) 103107.
- [32] J. Lancaster and A. Mitra, *Phys. Rev. E* **81**, 061134 (2010).
- [33] J.-M. Stéphan, *J. Stat. Mech.: Theory Exp.* (2017) 103108.
- [34] M. Collura, A. De Luca, and J. Viti, *Phys. Rev. B* **97**, 081111(R) (2018).
- [35] G. Misguich, N. Pavloff, and V. Pasquier, *SciPost Phys.* **7**, 25 (2019).
- [36] M. Schiró, *Phys. Rev. B* **81**, 085126 (2010).
- [37] R. Vasseur, K. Trinh, S. Haas, and H. Saleur, *Phys. Rev. Lett.* **110**, 240601 (2013).
- [38] F. Schwarz, I. Weymann, J. von Delft, and A. Weichselbaum, *Phys. Rev. Lett.* **121**, 137702 (2018).
- [39] T. Giamarchi, *Quantum Physics in One Dimension* (Oxford University Press, Oxford, 2004).
- [40] I. Safi and H. J. Schulz, *Phys. Rev. B* **52**, R17040 (1995).
- [41] D. L. Maslov and M. Stone, *Phys. Rev. B* **52**, R5539 (1995).
- [42] I. Safi, *Eur. Phys. J. B* **12**, 451 (1999).
- [43] J. P. Das, C. Chowdhury, and G. S. Setlur, *Theor. Math. Phys.* **199**, 736 (2019).
- [44] For particle transport in charge neutral systems, the conductance quantum becomes $G = e^2/h \rightarrow 1/h$.
- [45] S. Krinner, D. Stadler, D. Husmann, J.-P. Brantut, and T. Esslinger, *Nature (London)* **517**, 64 (2015).
- [46] K. Yamamoto, Y. Ashida, and N. Kawakami, *Phys. Rev. Research* **2**, 043343 (2020).
- [47] G. Vidal, *Phys. Rev. Lett.* **91**, 147902 (2003).
- [48] M. Zwolak and G. Vidal, *Phys. Rev. Lett.* **93**, 207205 (2004).
- [49] G. Vidal, *Phys. Rev. Lett.* **98**, 070201 (2007).
- [50] A. Mitra, *Annu. Rev. Condens. Matter Phys.* **9**, 245 (2018).
- [51] T. Sabetta and G. Misguich, *Phys. Rev. B* **88**, 245114 (2013).
- [52] E. Langmann, J. L. Lebowitz, V. Mastropietro, and P. Moosavi, *Commun. Math. Phys.* **349**, 551 (2017).
- [53] D. M. Weld, P. Medley, H. Miyake, D. Hucul, D. E. Pritchard, and W. Ketterle, *Phys. Rev. Lett.* **103**, 245301 (2009).
- [54] J.-y. Choi, S. Hild, J. Zeiher, P. Schauß, A. Rubio-Abadal, T. Yefsah, V. Khemani, D. A. Huse, I. Bloch, and C. Gross, *Science* **352**, 1547 (2016).
- [55] M. A. Nichols, L. W. Cheuk, M. Okan, T. R. Hartke, E. Mendez, T. Senthil, E. Khatami, H. Zhang, and M. W. Zwierlein, *Science* **363**, 383 (2019).
- [56] The parity symmetry P is associated with the phase transformation $b_q \rightarrow ib_q$ and $b_q^\dagger \rightarrow -ib_q^\dagger$, while the time reversal symmetry T corresponds simply to the conjugation $i \rightarrow -i$. The model is PT symmetric in the sense that the Hamiltonian defined in Eq. (4) does not commute with the generators of each symmetry independently but only with their product.
- [57] J. Lancaster, E. Gull, and A. Mitra, *Phys. Rev. B* **82**, 235124 (2010).
- [58] S. R. White, *Phys. Rev. Lett.* **69**, 2863 (1992).
- [59] B. Rauer, P. Grišins, I. E. Mazets, T. Schweigler, W. Rohringer, R. Geiger, T. Langen, and J. Schmiedmayer, *Phys. Rev. Lett.* **116**, 030402 (2016).
- [60] S. Erne, R. Bücke, T. Gasenzer, J. Berges, and J. Schmiedmayer, *Nature (London)* **563**, 225 (2018).
- [61] E. M. Graefe, H. J. Korsch, and A. E. Niederle, *Phys. Rev. Lett.* **101**, 150408 (2008).